

Potential volcanic impacts on future climate variability

Article

Accepted Version

Bethke, I., Outten, S., Otterå, O. H., Hawkins, E. ORCID: <https://orcid.org/0000-0001-9477-3677>, Wagner, S., Sigl, M. and Thorne, P. (2017) Potential volcanic impacts on future climate variability. *Nature Climate Change*, 7 (11). pp. 799-805. ISSN 1758-678X doi: <https://doi.org/10.1038/nclimate3394> Available at <https://centaur.reading.ac.uk/74097/>

It is advisable to refer to the publisher's version if you intend to cite from the work. See [Guidance on citing](#).

Published version at: <http://dx.doi.org/10.1038/nclimate3394>

To link to this article DOI: <http://dx.doi.org/10.1038/nclimate3394>

Publisher: Nature Publishing Group

All outputs in CentAUR are protected by Intellectual Property Rights law, including copyright law. Copyright and IPR is retained by the creators or other copyright holders. Terms and conditions for use of this material are defined in the [End User Agreement](#).

www.reading.ac.uk/centaur

CentAUR

Central Archive at the University of Reading

Reading's research outputs online

1 **Potential volcanic impacts on future climate variability**

2

3 **Ingo Bethke¹, Stephen Outten², Odd Helge Otterå¹, Ed Hawkins³, Sebastian Wagner⁴,**
4 **Michael Sigl^{5,6}, Peter Thorne⁷**

5

6 *¹Uni Research Climate, Bjerknes Centre for Climate Research, Bergen, Norway*

7 *²Nansen Environmental and Remote Sensing Center, Bjerknes Centre for Climate Research,*
8 *Bergen, Norway*

9 *³NCAS-Climate, Department of Meteorology, University of Reading, Reading, UK*

10 *⁴Institute for Coastal Research, Helmholtz-Zentrum Geesthacht, Germany*

11 *⁵Laboratory of Environmental Chemistry, Paul Scherrer Institute, Switzerland*

12 *⁶Oeschger Centre for Climate Change Research, University of Bern, Switzerland*

13 *⁷Irish Climate Analysis and Research Units, Department of Geography, National University*
14 *of Ireland Maynooth, Ireland*

15

16

17 **Corresponding author**

18 Correspondence to: Ingo Bethke <ingo.bethke@uni.no>

19 **New ice-core records¹ highlight large variations in volcanism over the past 2,500 years,**
20 **causing variations in past climate². Most state-of-the-art climate projections for the 21st**
21 **century under-sample future volcanic effects by not representing the range of plausible**
22 **future volcanic activity^{3,4,5}. Here we explore sixty possible volcanic futures, each**
23 **consistent with the ice-core records, applied to 21st century projections. Their inclusion**
24 **notably enhances the climate variability on annual-to-decadal time scales. We find a 50%**
25 **increase both in annual-mean global temperature variability and in decades with a**
26 **negative global temperature trend. Volcanic activity also impacts probabilistic**
27 **projections of global radiation, sea level, ocean circulation, and sea ice variability; and**
28 **has local-scale detectible impacts. The episodic forcing only weakly affects the long-term**
29 **trends and occurrence of warm years, making it unlikely to mitigate long-term global**
30 **warming impacts. Conversely, the effects on variance and extremes are substantial and**
31 **expected to be important for many adaptation decisions and risk assessments⁶. We thus**
32 **conclude that including plausible volcanic uncertainty is both possible and important in**
33 **future climate assessments.**

34

35 Volcanism has been a major driver of past climate variability² and will continue to affect
36 future climate alongside human influences⁷. Explosive volcanic eruptions warm the
37 stratosphere⁸, cool the troposphere⁹, cause changes in the hydrological cycle^{10,11}, and trigger
38 modifications of atmospheric circulation that give rise to large regional climate responses¹².
39 The instrumental period covering the last 150 years has been relatively volcanically quiescent,
40 and it is therefore tempting to ascribe potential volcanism a minor role in future climate
41 impact and risk assessments. In a millennial perspective, however, there have been periods
42 with considerably stronger volcanic activity¹ (Supplementary Fig. 1). Clustered occurrence of
43 strong tropical eruptions has contributed to sustained cold periods such as the Little Ice Age¹³,

44 where the longer-term climate impacts are mediated through ocean heat content anomalies¹⁴
45 and ocean circulation changes¹⁵⁻¹⁷ that also affect global and regional sea level¹⁸ and sea ice
46 conditions^{13,15}.

47

48 Because volcanic eruptions are unpredictable events, they have generally been excluded from
49 21st century climate projection protocols. Most recent projections either specify future
50 volcanic forcing as zero or a constant background value⁵, while considerations of more
51 realistic volcanic effects have been limited to idealised eruption scenarios, repeating recent
52 volcanic activity in near-future simulations^{3,19}. Herein we explore whether a more complete
53 representation of volcanic forcing uncertainty that considers a range of volcanic forcing
54 possibilities will have an impact on important aspects of probabilistic 21st century projections
55 increasingly being used for adaptation planning purposes. The risk from not realistically
56 accounting for volcanic forcing effects is that critical possible future outcomes are being
57 discounted and mal-adaptation ensues.

58 The possibility of utilizing stochastic volcanic forcing in projections has been recognised in
59 previous studies²⁰ and underscored in the latest assessment report of the Intergovernmental
60 Panel on Climate Change²¹. Increasing computational power facilitating large ensemble
61 simulations²², together with improved reconstructions of past volcanic activity¹ that allow for
62 a better statistical characterisation^{7,20}, make it timely to revisit the question of volcanic effects
63 on 21st century climate projections. We start by deriving plausible future volcanic forcings
64 (Fig. 1) by sampling from reconstructed volcanic activity of the last 2,500 years¹
65 (Supplementary Fig. 1). We next perform three 21st century simulation ensembles with the
66 Norwegian Earth System Model (NorESM)²³, that use the same mid-range anthropogenic
67 forcing scenario RCP4.5²⁴ but differ in their volcanic forcing: a 60-member ensemble using
68 plausible stochastic volcanic forcing (VOLC); a 60-member reference ensemble using zero
69 volcanic forcing (NO-VOLC); and a 20-member ensemble using 1850–2000 averaged
70 volcanic forcing²⁵ (VOLC-CONST). NO-VOLC and VOLC-CONST are the two approaches
71 that were adopted across the group of models contributing 21st century projections to the
72 Coupled Model Intercomparison Project phase 5 (CMIP5)²⁶. Hence we consider both as
73 useful counterfactual cases here to aid reader interpretation of possible limitations in existing
74 21st century projection runs. Specifically, we assessed the volcanic influence on the climate
75 variability and means of future projections by comparing our three ensembles for several
76 societally relevant diagnostics.

77

78 We start by examining the impact of future volcanic activity on Global-Mean Surface Air
79 Temperature (GMST) – an integrated climate change indicator of particular relevance to
80 mitigation decision making. Figure 2a shows annual-mean GMST changes over the course of
81 the 21st century as simulated in the three ensembles. The effect of volcanic forcing on the
82 ensemble mean temperature (thick solid lines) is modest, amounting to a 5% reduction of the

83 centennial GMST change projected under RCP4.5, with VOLC and VOLC-CONST being
84 slightly cooler than NO-VOLC throughout the post-2005 period as expected from the first-
85 order response to volcanic forcing. Near-term GMST projections for the 2016–2035 period
86 (Fig. 2b) exhibit only a small (0.05 K) reduction in mean response in VOLC and VOLC-
87 CONST, with an increased skew in VOLC leading to a 0.1 K shift in the lower distribution
88 tail. As a result, the 1.5°C warming target of the Paris agreement COP-21²² is exceeded on
89 average two years later in VOLC and VOLC-CONST (Supplementary Table 1), with the
90 upper distribution tail of VOLC being shifted by twice that amount (Fig. 2c). Models which
91 did not include constant background forcing in their standard 21st century simulations
92 prepared for CMIP5 are thus overly-pessimistic as to the likely time until different warming
93 thresholds are reached.

94

95 Over the course of the simulation period, the ensemble mean difference grows, eventually
96 saturating just below 0.1 K around 2040 (Fig. 2a), after which the means are well separated.
97 The delay highlights the role of slow-response components, particularly the ocean^{14,15}, in
98 aggregating the global response to episodic volcanic forcing. The general correspondence of
99 the VOLC and VOLC-CONST ensemble shows that the application of a time-invariant
100 background forcing adequately accounts for long-term aspects of volcanic impacts in the
101 ensemble mean projections. One could use plausible low and high background values To
102 further account for projection uncertainty stemming from uncertainty in the centennial-mean
103 volcanic forcing, (Fig. 1c and Supplementary Fig. 1). However, this would fail to capture the
104 response to episodic volcanic forcing and attendant impacts on annual-to-decadal variability
105 and extremes.

106

107 The interannual uncertainty range (5-95% ensemble spread) in annual-mean GMST is
108 inflated by more than 50% (from 0.3 to 0.5 K) in VOLC relative to NO-VOLC (Fig. 2a – red
109 vs blue shading; individual VOLC ensemble member GMST are shown in Supplementary
110 Fig. 9). Consistent with a tropospheric cooling response, the change in ensemble spread in
111 VOLC relative to NO-VOLC is skewed towards lower GMST, leaving the higher bound
112 largely unaltered (Fig. 2d). Reductions in frequency of extremely warm years are generally
113 small, whereas increases in frequency of extremely cold years – relative to the moving
114 average or ‘present-day’ climate at any point – are much more substantial. In contrast, the
115 application of a constant background forcing merely shifts the distribution of VOLC-CONST
116 relative to NO-VOLC, overestimating the reduction of warm years and underestimating the
117 increase of cold years.

118

119 Decadal-scale GMST series are even more affected by future volcanic forcing uncertainty
120 than annual temperatures (Fig. 3a). The distribution of the decadal means – with the global
121 warming trend removed prior to the analysis – is considerably wider for VOLC than for NO-
122 VOLC, with roughly a doubling in standard-deviation (Fig. 3b and Supplementary Table 1).
123 Anomalously cold decades become more frequent at the expense of ‘normal’ and, to a lesser
124 degree, anomalously warm decades. As for decadal means, the spread in decadal trends is
125 significantly wider for VOLC than for NO-VOLC (Fig. 3c). Occurrences of decades with
126 negative GMST trend become more frequent if accounting for volcanic forcing, with the
127 probability increasing from 10% in NO-VOLC to more than 16% in VOLC (Fig. 3d).
128 Conversely, the widening of the upper tail of the decadal trend distribution (Fig. 3c) indicates
129 enhanced probability of decadal-scale warming surges, due to the rebound of GMST after
130 volcanic induced cooling has reached its maximum (cf. Supplementary Fig. 4). The
131 probability of decades with negative GMST trend more than doubles from 4% to 10% (Fig.

132 3e) if the analysis is limited to the first half of the century – before the stabilization period of
133 RCP4.5 – suggesting that the relative impact is sensitive to other forcings and depends on the
134 anthropogenic scenario. Volcanic induced cooling becomes increasingly important in
135 facilitating neutral or negative temperature trends on longer timescales on which natural
136 internal variability effects such as ENSO are no longer sufficient to offset anthropogenic
137 forcings (Fig. 3f,g).

138

139 That volcanic influence is not limited to GMST projections becomes evident from assessing
140 selected global and large-scale climate indicators that all have previously been found to be
141 sensitive to volcanism^{11,15-18} (Fig. 4 and Supplementary Table 1). The radiative forcing at the
142 top of the atmosphere is reduced by 0.05 W/m^2 on average (Fig. 4a), while its decadal
143 standard-deviation, including the anthropogenic RCP4.5 signal, is increased by 80% in
144 response to volcanic forcing. The distribution of decadal radiative anomalies is widened with
145 a skew towards lower values (Fig. 4b) and a slight occurrence of more positive extremes
146 resulting from reduced radiative surface cooling in post-eruption years. Global sea level rise
147 is on average slowed by 4% (relative to RCP4.5) in VOLC compared to NO-VOLC (Fig. 4c)
148 as a direct consequence of reduced heat uptake by the oceans. The distribution of decadal sea
149 level anomalies is significantly widened (doubling of standard-deviation after subtracting
150 global warming trend) with the lower uncertainty tail being affected most (Fig. 4d). Contrary
151 to GMST, the volcanic forcing is generally not strong enough to halt global steric sea level
152 rise by offsetting anthropogenic driven ocean warming on decadal and longer time scales.
153 Asian summer monsoon precipitation shows consistent, albeit small reductions (Fig. 4e), with
154 all decades featuring lower ensemble means, and a 20% overall increase in ensemble
155 standard-deviation (Fig. 4f). The Atlantic Meridional Overturning Circulation (AMOC)
156 evaluated at 26°N shows a relative strengthening of 0.2 Sv in VOLC compared to NO-VOLC

157 (Fig. 4g), with all decades exhibiting increased ensemble means, and a 20% overall increase
158 in ensemble standard-deviation (Fig. 4h). Similarly, Arctic sea ice volume shows a 1-2%
159 relative increase for most decades (Fig. 4i) and a 15% increase in ensemble standard-
160 deviation (Fig. 4j), with more overlap between the spread of subsequent decades in VOLC
161 compared to NO-VOLC indicating enhanced probability for a temporary halt in Arctic sea ice
162 decline.

163

164 To address if the inclusion of volcanic forcing variability has local implications we
165 performed a time-of-emergence (ToE) analysis²⁷ on seasonally averaged surface air
166 temperature (Fig. 5). The ToE is formally defined as the mean time at which the signal of
167 climate change emerges from the noise of natural climate variability (see Methods). The
168 simulated impact of volcanic forcing variability on the ToE changes is distinct but small. The
169 ToE is delayed almost everywhere as a consequence of the inclusion of volcanic forcing (Fig.
170 5a,b). The distribution of the simulated delay is strongly skewed and indicates a ToE delay of
171 up to a decade in some locations, and of three years on average (Fig. 5c,d).

172

173 Our results highlight the importance of representing volcanic forcing uncertainty in
174 probabilistic future climate projections, in particular for risk assessments with focus on
175 variability and certain extremes. Counter to earlier findings of destructive interference of
176 volcanic forcing with internal climate variability modes¹⁶, our stochastic volcanic forcing
177 generally amplifies the annual-to-decadal scale climate variability in our model. A sharp
178 increase in simulated decades with negative GMST trend exemplifies the effect of volcanic
179 forcing uncertainty on projections of climate extremes. While volcanic-induced GMST trends
180 have arguably limited direct human impacts, similar effects on other extremes – such as
181 Arctic sea ice extent or reduced monsoon precipitation – lead to direct socioeconomic

182 consequences. Extreme volcanic activity can potentially cause extended anomalously cold
183 periods. This will, however, not help to mitigate long-term global warming impacts as the
184 surface climate is likely to rebound, leaving its long-term trajectory virtually unaltered (Fig.
185 2a, yellow curve).

186
187 This study is a first step towards incorporating current knowledge on global volcanic activity
188 in probabilistic future climate projections in realistic and systematic ways. It serves as a
189 proof-of-concept for a statistical representation of potential volcanism in 21st century climate
190 projections and demonstrates the importance of such a representation for the projections of
191 future climate variability. Our ensemble analysis, based on a single model and a single
192 anthropogenic scenario, provides only a conditional assessment of the volcanic contribution
193 to climate projection uncertainty²⁸. Additional uncertainties in the volcanic forcing
194 reconstruction, in other external forcings and in the model (details in Supplementary
195 Information) warrant further experiments. Since simulated regional impacts are less distinct
196 than global impacts and have larger model uncertainty²⁸, quantifying volcanic impacts on
197 regional climate projections and their socio-economic aspects should be a priority of future
198 work. Improved characterisation of past volcanic forcing, improved representation of
199 volcanic impact in models, and coordinated multi-model efforts using the same plausible
200 forcings are essential ingredients for advancing the utilisation of volcanism information in
201 future climate assessments. The newly established Model Intercomparison Project on climatic
202 response to Volcanic forcing (VolMIP)²⁹ presents the ideal platform for integrating these
203 efforts.

204 References

- 205 1. Sigl, M. *et al.* Timing and climate forcing of volcanic eruptions for the past 2,500 years.
206 *Nature* **523**, 543–549 (2015).
- 207 2. Schurer, A. P., Tett, S. F. B. & Hegerl, G. C. Small influence of solar variability on
208 climate over the past millennium. *Nat. Geosci.* **7**, 104–108 (2014).
- 209 3. Hansen, J. *et al.* Global climate changes as forecast by Goddard Institute for Space
210 Studies three-dimensional model. *J. Geophys. Res.* **93**, 9341 (1988).
- 211 4. Gregory, J. M. Long-term effect of volcanic forcing on ocean heat content. *Geophys. Res.*
212 *Lett.* **37** (2010).
- 213 5. O’Neill, B. C. *et al.* The Scenario Model Intercomparison Project (ScenarioMIP) for
214 CMIP6. *Geosci. Model Dev.* **9**, 3461–3482 (2016).
- 215 6. Oppenheimer, C. Climatic, environmental and human consequences of the largest known
216 historic eruption: Tambora volcano (Indonesia) 1815. *Prog. Phys. Geogr.* **27**, 230–259
217 (2003).
- 218 7. Hyde, W. T. & Crowley, T. J. Probability of Future Climatically Significant Volcanic
219 Eruptions. *J. Clim.* **13**, 1445–1450 (2000).
- 220 8. Parker, D. E. & Brownscombe, J. L. Stratospheric warming following the El Chichón
221 volcanic eruption. *Nature* **301**, 406–408 (1983).
- 222 9. Robock, A. & Mao, J. The Volcanic Signal in Surface Temperature Observations. *J. Clim.*
223 **8**, 1086–1103 (1995).
- 224 10. Iles, C. E. & Hegerl, G. C. Systematic change in global patterns of streamflow following
225 volcanic eruptions. *Nat. Geosci.* **8**, 838–842 (2015).
- 226 11. Liu, F. *et al.* Global monsoon precipitation responses to large volcanic eruptions. *Sci. Rep.*
227 **6**, 24331 (2016).

- 228 12. Shindell, D. T., Schmidt, G. A., Mann, M. E. & Faluvegi, G. Dynamic winter climate
229 response to large tropical volcanic eruptions since 1600. *J. Geophys. Res* **109**, D05104
230 (2004).
- 231 13. Miller, G. H. *et al.* Abrupt onset of the Little Ice Age triggered by volcanism and
232 sustained by sea-ice/ocean feedbacks. *Geophys. Res. Lett.* **39** (2012).
- 233 14. Gleckler, P. J. *et al.* Volcanoes and climate: Krakatoa's signature persists in the ocean.
234 *Nature* **439**, 675 (2006).
- 235 15. Stenchikov, G. *et al.* Volcanic signals in oceans. *J. Geophys. Res.* **114**, D16104 (2009).
- 236 16. Swingedouw, D. *et al.* Bidecadal North Atlantic ocean circulation variability controlled
237 by timing of volcanic eruptions. *Nat. Commun.* **6**, 6545 (2015).
- 238 17. Otterå, O. H., Bentsen, M., Drange, H. & Suo, L. External forcing as a metronome for
239 Atlantic multidecadal variability. *Nat. Geosci.* **3**, 688–694 (2010).
- 240 18. Church, J. A., White, N. J. & Arblaster, J. M. Significant decadal-scale impact of volcanic
241 eruptions on sea level and ocean heat content. *Nature* **438**, 74–7 (2005).
- 242 19. Shiogama, H. *et al.* Possible Influence of Volcanic Activity on the Decadal Potential
243 Predictability of the Natural Variability in Near-Term Climate Predictions. *Adv. Meteorol.*
244 **2010**, 1–7 (2010).
- 245 20. Ammann, C. M. & Naveau, P. A statistical volcanic forcing scenario generator for
246 climate simulations. *J. Geophys. Res.* **115**, D05107 (2010).
- 247 21. Kirtman, B., S.B. Power, J.A. Adedoyin, G.J. Boer, R. Bojariu, I. Camilloni, F.J. Doblas-
248 Reyes, A.M. Fiore, M. Kimoto, G.A. Meehl, M. Prather, A. Sarr, C. Schar, R. Sutton, G.J.
249 van Oldenborgh, G. Vecchi and H.J. Wang, 2013: Near-term Climate Change: Projections
250 and Predictability. In: *Climate Change 2013: The Physical Science Basis. Contribution of*
251 *Working Group I to the Fifth Assessment Report of the Intergovernmental Panel on*
252 *Climate Change*

- 253 22. Mitchell, D. *et al.* Realizing the impacts of a 1.5 °C warmer world. *Nat. Clim. Chang.* **6**,
254 735–737 (2016).
- 255 23. Bentsen, M. *et al.* The Norwegian Earth System Model, NorESM1-M – Part 1:
256 Description and basic evaluation of the physical climate. *Geosci. Model Dev.* **6**, 687–720
257 (2013).
- 258 24. Vuuren, D. P. *et al.* The representative concentration pathways: an overview. *Clim.*
259 *Change* **109**, 5–31 (2011).
- 260 25. Ammann, C. M., Meehl, G. A., Washington, W. M. & Zender, C. S. A monthly and
261 latitudinally varying volcanic forcing dataset in simulations of 20th century climate.
262 *Geophys. Res. Lett.* **30**, 1657 (2003).
- 263 26. Taylor, K. E. *et al.* An Overview of CMIP5 and the Experiment Design. *Bull. Am.*
264 *Meteorol. Soc.* **93**, 485–498 (2012).
- 265 27. Hawkins, E. & Sutton, R. Time of emergence of climate signals. *Geophys. Res. Lett.* **39**
266 (2012).
- 267 28. Hawkins, E. & Sutton, R. The Potential to Narrow Uncertainty in Regional Climate
268 Predictions. *Bull. Am. Meteorol. Soc.* **90**, 1095–1107 (2009).
- 269 29. Zanchettin, D. *et al.* The Model Intercomparison Project on the climatic response to
270 Volcanic forcing (VolMIP): experimental design and forcing input data for CMIP6.
271 *Geosci. Model Dev.* **9**, 2701–2719 (2016).

272 Online Methods

273 **Historical volcanic data utilised.**

274 We consider multiple ice-cores from Greenland and Antarctica utilising the sulphate
275 contained in the ice-core as a proxy for explosive volcanic activity of the past 2,500 years¹.

276 Although the approach is subject to uncertainties arising from issues such as: dating
277 uncertainties; scaling of sulphate peaks to changes in stratospheric aerosol loads;
278 representativeness of different regions over Greenland and Antarctica for volcanic sulphate
279 emissions; and discrimination of single tropical versus two individual high latitude eruptions,
280 it provides an insight into the plausible range of magnitude and temporal structure of future
281 volcanic eruptions. Ice-core records, however, do omit small volcanic events which may
282 nevertheless have some impacts on climate³⁰. Earlier reconstructions³¹⁻³³ of past volcanic
283 eruptions for the last millennium AD show similar temporal evolution and timing, albeit with
284 differences in magnitude. The use of multiple cores in our reconstruction is thought to
285 improve on earlier overestimates of, in particular, larger eruptions³⁴ such as the Samalas
286 eruption in 1257³⁵. The series represents the longest currently available annually-resolved
287 continuous series, making it particularly suitable for our study. The series provides
288 information on timing, magnitude of sulphur injection and location (tropical versus
289 extratropical in respective hemisphere) of a total of 283 eruption events for which ice-core
290 sulphate concentrations exceeded a detection threshold (approximately 1/3 of the strength of
291 a tropical eruption such as Pinatubo in 1991) defined by the natural variability of non-
292 volcanic sulphate in the ice. Eruptions from Iceland and Alaska are expected to be
293 overrepresented in this dataset due to their proximity to Greenland. Anthropogenic SO₂
294 emissions predominantly from the United States and Europe peaking in the 1970-1980s (i.e.,
295 ‘global dimming’³⁶) mask volcanic sulphate contributions in Greenland ice cores during parts
296 of the 20th century³⁷, hampering detection and quantification of volcanic sulphate deposition
297 for eruptions such as El Chichón in 1982. Nevertheless, that the last 150 years were
298 comparatively ‘quiet’ is supported by the ice-cores from Antarctica, which are not subject to
299 significant human sulphate pollution and suggest that the stratospheric loadings between
300 1850–2000 CE were 30% lower compared to the 1–2000 CE average³⁴.

301

302 **Stochastic forcing generation.**

303 We generated plausible future eruption chronologies by resampling the past volcanic activity
304 described in the prior section (code in Supplementary Information). For each month of the
305 period 2006 to 2099, we draw random numbers from a uniform distribution to test whether
306 one or more of the 283 eruption events in Sigl et al.¹ were triggered in that ensemble member
307 on that date. For the test we assumed a constant eruption probability of $1/(2500*12)$, which is
308 the probability of randomly picking the exact month from the 2,500 year record when a
309 specific eruption event occurred. By repeating this procedure for all months and all forcing
310 members, we obtained 60 unique plausible future eruption chronologies for the 21st century
311 (using the CMIP5 standard period 2006–2099), with statistics that resemble those of the
312 historical reconstruction (Supplementary Fig. 2).

313

314 We then translated the plausible 21st century eruption chronologies into model forcing
315 ancillaries. First, we estimated peak stratospheric sulphate aerosol loadings by scaling the ice-
316 core depositions of the individual events using established scaling relations³¹. The peak
317 loadings were then used to scale the generic dispersal evolution of volcanic aerosols – one
318 generic evolution for tropical and one for extratropical eruptions (Supplementary Fig. 6) –
319 that are applied in the model²⁵. We validated this approach by comparing ice-core based
320 historical forcing, that we constructed in the same way, to the model's default historical
321 forcing (see section 2 in Supplementary Information for details). The comparison reveals no
322 systematic bias, and a time-mean difference of less than 10% (Supplementary Fig. 7).

323

324 **Implementation and validation of volcanic forcing.**

325 The ice-core based reconstruction of Sigl et al.¹ provides global estimates for maximum
326 stratospheric volcanic aerosol load following the volcanic eruptions and whether the
327 eruptions were tropical or NH/SH extratropical. To translate this information into model
328 forcing, we analysed the data set of Ammann et al.²⁵ who used a transport model to estimate
329 the spatio-temporal dispersal of stratospheric volcanic aerosols for the 20th century.
330 We found that their dispersal evolution can be approximated by three shape functions
331 (Supplementary Fig. 6) - one for tropical and two for extratropical NH/SH eruptions - that
332 only depend on pressure, latitude and time since eruption start. We derived the final model
333 forcing by scaling the shape functions with the maximum aerosol load estimated from the ice-
334 core reconstruction. Our forcing implementation thus does not consider the seasonal effects
335 on dispersal of volcanic aerosols discussed in Ammann et al.²⁵.

336

337 We compare the volcanic forcing that we generated from the ice-core data with the Ammann
338 et al.²⁵ forcing for the period 1850–2000 in order to assess whether our model forcing is
339 biased towards low or high values (Supplementary Fig. 7). While the timing and forcing
340 magnitudes match well for some eruptions (e.g., 1883–Krakatau, 1963–Agung and 1991–Mt.
341 Pinatubo), they differ for others (e.g., 1902–Santa Maria, 1980–Mt. St. Helens and 1982–El
342 Chichón) partly for reasons previously outlined. Despite discrepancies for individual
343 eruptions, however, no systematic differences in size or frequency distributions are seen and
344 the time-means – 1.15 Tg versus 1.22 Tg volcanic aerosol load in ice-core based versus
345 Ammann et al.²⁵ forcing – match well.

346

347 **Model configuration.**

348 We performed all simulations with the medium resolution configuration of the Norwegian
349 Earth System Model version 1 (NorESM1-M)^{23,38}, a state-of-the-art climate model that

350 provided input to the fifth Coupled Model Intercomparison Project (CMIP5)²⁶. We used the
351 exact configuration that was employed in performing those CMIP5 runs. NorESM1-M is
352 based on the Community Climate System Model version 4³⁹. Important modifications to the
353 latter are the employment of an isopycnic coordinate ocean component, improving the
354 conservation and transformation properties of water masses, and the addition of a more
355 advanced aerosol-cloud chemistry treatment in the atmosphere component. The land and sea
356 ice components are adopted in their original form.

357

358 The atmosphere and land components are configured on a regular 1.9°x2.5° horizontal grid,
359 while the ocean and sea-ice components are configured on a 1° curvilinear horizontal grid
360 with the northern pole singularity shifted over Greenland. The atmospheric component
361 features 26 hybrid sigma-pressure levels extending to 3 hPa. The ocean component features a
362 stack of 51 isopycnic layers, with a variable depth bulk mixed-layer on top.

363

364 NorESM1-M has been used to study the effect of major extratropical eruptions^{40,41}, where
365 volcanic sulphur dioxide was directly injected into the atmosphere and subsequent oxidation
366 to sulphate aerosols was simulated by the model. This approach is not applicable here as it
367 would require a statistical model for sulphur emissions that can provide exact geographic
368 locations, injection rates as well as injection heights. Hence, we prescribe volcanic sulphate
369 aerosol concentrations, following the approach used for NorESM's CMIP5 simulations²³,
370 where the model reads a mass distribution of stratospheric volcanic sulphate aerosols
371 (Supplementary Fig. 6), which is converted to number concentrations – assuming a fixed,
372 log-normal size distribution – and combined with prognostic sulphate before being passed to
373 the radiation code.

374

375 **Model spin-up and sensitivity test.**

376 We generated starting conditions for the 21st century simulations by performing a 26-year
377 spinup experiment, which we spawned off three simulation sets with 20 members each from
378 the year 1980 states of NorESM's three historical CMIP5 simulations²³. Initial spread within
379 each set was generated through adding small ($O(10^{-6}K)$) noise to the ocean mixed layer
380 temperatures. The total of 60 members were integrated to the end of year 2005, after which
381 time the ensemble spread had reached saturation on most relevant diagnostics^{42,43}, such as
382 AMOC variability (Supplementary Fig. 8). As a result, the covariability between individual
383 members of our 21st century simulations is very close to zero.

384

385 We performed a 60-member spin-up ensemble for the post-Mt. Pinatubo eruption period
386 1990–2005, that is identical to the first one but with the forcing of the Mt. Pinatubo eruption
387 removed. Analysing the differences of the two ensembles allowed us to verify the model's
388 sensitivity to volcanic forcing (details in Supplementary Information).

389

390 **Bootstrap confidence intervals.**

391 We used empirical bootstrapping⁴⁴ to assess statistical robustness. For each test, we generated
392 10,000 bootstrap samples by resampling the original data with replacement. We then
393 performed our analysis on each bootstrap sample and derived 5-95% confidence intervals by
394 ranking the results. In the generation of the bootstrap sample, we treated the data from
395 individual simulations as contiguous blocks⁴⁵ in order to account for effects of
396 autocorrelation along the temporal dimension. The autocorrelation along the ensemble
397 dimension was zero by construction.

398

399 **Pre-industrial (PI) reference climate.**

400 We show all diagnostics relative to a pre-industrial reference climate to put the volcanic
401 impacts into a climate change perspective. We computed the reference climatology from the
402 500-year-long pre-industrial control simulation that NorESM contributed to CMIP5^{23,26}. This
403 simulation used external forcings fixed at 1850 levels and no volcanic forcing.

404

405 **Time-of-Emergence (ToE) analysis.**

406 Our ToE analysis on seasonally averaged surface air temperature follows Hawkins &
407 Sutton²⁷. We define ToE as the earliest occurrence where the signal-to-noise ratio exceeds the
408 value 2 (climate change signal is distinguishable from zero at a 95% confidence level). For
409 each simulation member, we estimated the signal by regressing the local time series onto the
410 corresponding global mean time series. We then estimated the noise, i.e., unforced internal
411 climate variability, from standard-deviations of a 500 year-long pre-industrial control
412 simulation²³ that was run with the same model configuration as used in this study. The
413 obtained ToEs were averaged over the respective NO-VOLC and VOLC ensemble. The
414 analysis was performed for extended boreal winter (October-March) and boreal summer
415 (April-September) averages.

416

417 **Code availability.**

418 The code for the generation of synthetic volcanic forcings is included in the Supplementary
419 Information. The Norwegian Earth System Model can be obtained by sending a request to
420 noresm-ncc@met.no.

421

422 **Data availability.**

423 The model output from this study and volcanic forcing ancillaries are available at
424 <https://doi.org/10.11582/2017.00006>

425 References

- 426 30. Santer, B. D. *et al.* Volcanic contribution to decadal changes in tropospheric temperature.
427 *Nat. Geosci.* **7**, 185–189 (2014).
- 428 31. Gao, C., Oman, L., Robock, A. & Stenchikov, G. L. Atmospheric volcanic loading
429 derived from bipolar ice cores: Accounting for the spatial distribution of volcanic
430 deposition. *J. Geophys. Res.* **112**, D09109 (2007).
- 431 32. Crowley, T. J. & Unterman, M. B. Technical details concerning development of a 1200 yr
432 proxy index for global volcanism. *Earth Syst. Sci. Data* **5**, 187–197 (2013).
- 433 33. Sigl, M. *et al.* A new bipolar ice core record of volcanism from WAIS Divide and NEEM
434 and implications for climate forcing of the last 2000 years. *J. Geophys. Res. Atmos.* **118**,
435 1151–1169 (2013).
- 436 34. Sigl, M. *et al.* Insights from Antarctica on volcanic forcing during the Common Era. *Nat.*
437 *Clim. Chang.* **4**, 6–10 (2014).
- 438 35. Vidal, C. M. *et al.* The 1257 Samalas eruption (Lombok, Indonesia): the single greatest
439 stratospheric gas release of the Common Era. *Sci. Rep.* **6**, 34868 (2016).
- 440 36. Wild, M. *et al.* From Dimming to Brightening: Decadal Changes in Solar Radiation at
441 Earth's Surface. *Science*. **308**, 847–850 (2005).
- 442 37. McConnell, J. R. *et al.* 20th-Century Industrial Black Carbon Emissions Altered Arctic
443 Climate Forcing. *Science*. **317**, 1381–1384 (2007).
- 444 38. Iversen, T. *et al.* The Norwegian Earth System Model, NorESM1-M – Part 2: Climate
445 response and scenario projections. *Geosci. Model Dev.* **6**, 389–415 (2013).
- 446 39. Gent, P. R. *et al.* The Community Climate System Model Version 4. *J. Clim.* **24**, 4973–
447 4991 (2011).

- 448 40. Pausata, F. S. R., Grini, A., Caballero, R., Hannachi, A. & Seland, Ø. High-latitude
449 volcanic eruptions in the Norwegian Earth System Model: the effect of different initial
450 conditions and of the ensemble size. *Tellus B* **67** (2015).
- 451 41. Pausata, F. S. R., Chafik, L., Caballero, R. & Battisti, D. S. Impacts of high-latitude
452 volcanic eruptions on ENSO and AMOC. *Proc. Natl. Acad. Sci.* **112** (2015).
- 453 42. Outten, S., Thorne, P., Bethke, I. & Seland, Ø. Investigating the recent apparent hiatus in
454 surface temperature increases: 1. Construction of two 30-member Earth System Model
455 ensembles. *J. Geophys. Res. Atmos.* **120**, 8575–8596 (2015).
- 456 43. Thorne, P., Outten, S., Bethke, I. & Seland, Ø. Investigating the recent apparent hiatus in
457 surface temperature increases: 2. Comparison of model ensembles to observational
458 estimates. *J. Geophys. Res. Atmos.* **120**, 8597–8620 (2015).
- 459 44. Efron, B. & Tibshirani, R. Bootstrap Methods for Standard Errors, Confidence Intervals,
460 and Other Measures of Statistical Accuracy. *Stat. Sci.* **1**, 54–75 (1986).
- 461 45. Carlstein, E. The Use of Subseries Values for Estimating the Variance of a General
462 Statistic from a Stationary Sequence. *Ann. Stat.* **14**, 1171–1179 (1986).

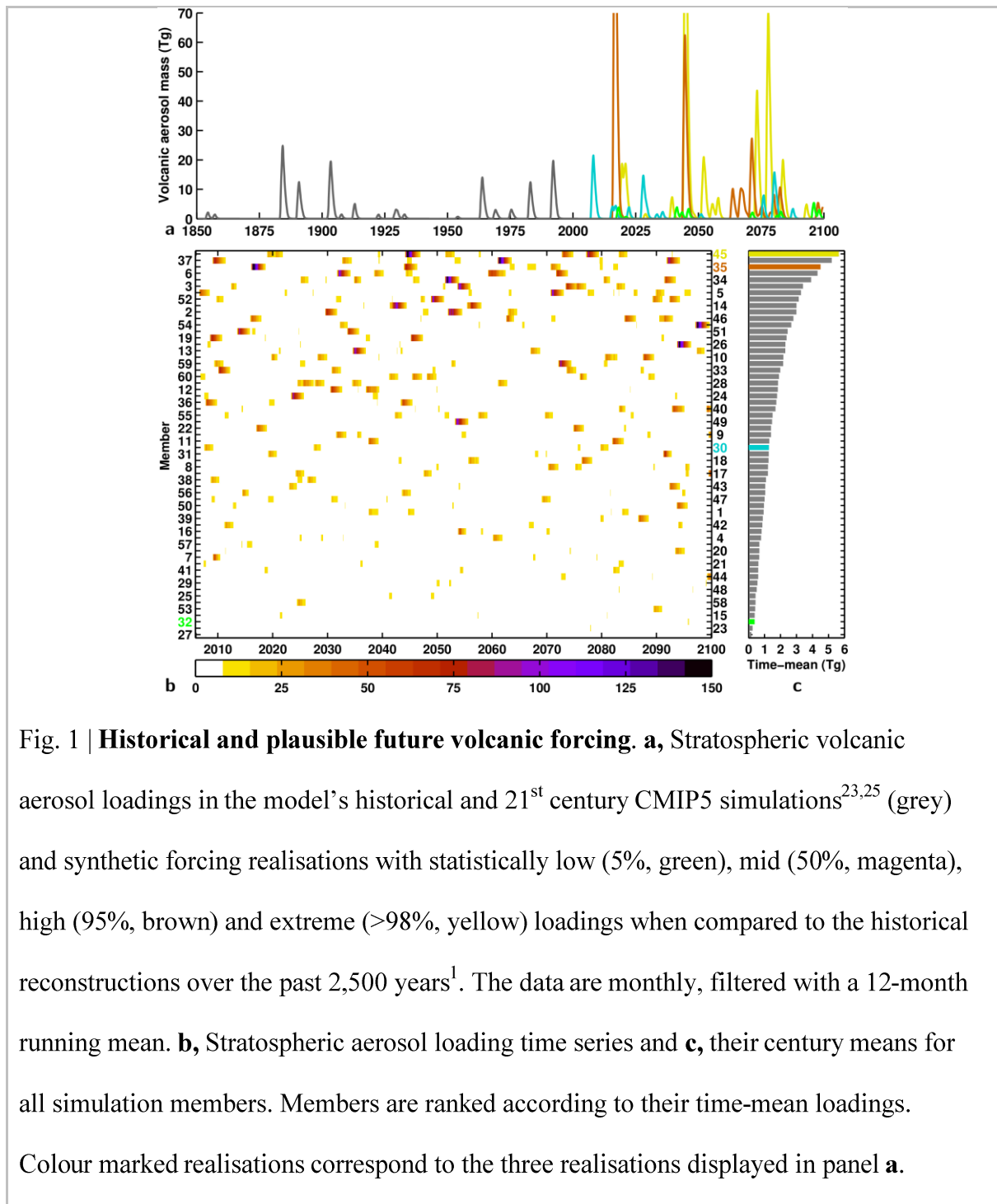
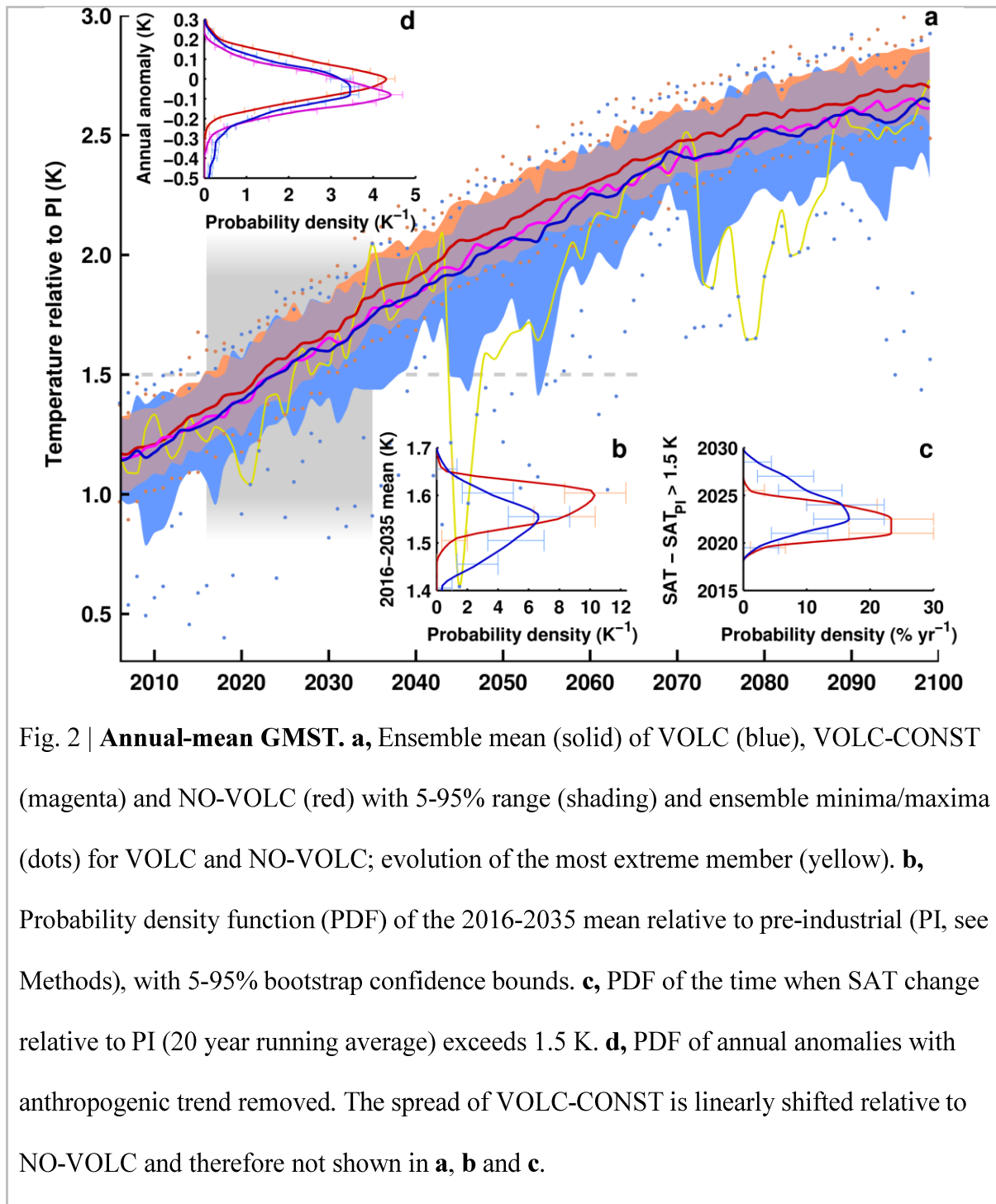


Fig. 1 | **Historical and plausible future volcanic forcing.** **a**, Stratospheric volcanic aerosol loadings in the model's historical and 21st century CMIP5 simulations^{23,25} (grey) and synthetic forcing realisations with statistically low (5%, green), mid (50%, magenta), high (95%, brown) and extreme (>98%, yellow) loadings when compared to the historical reconstructions over the past 2,500 years¹. The data are monthly, filtered with a 12-month running mean. **b**, Stratospheric aerosol loading time series and **c**, their century means for all simulation members. Members are ranked according to their time-mean loadings. Colour marked realisations correspond to the three realisations displayed in panel **a**.



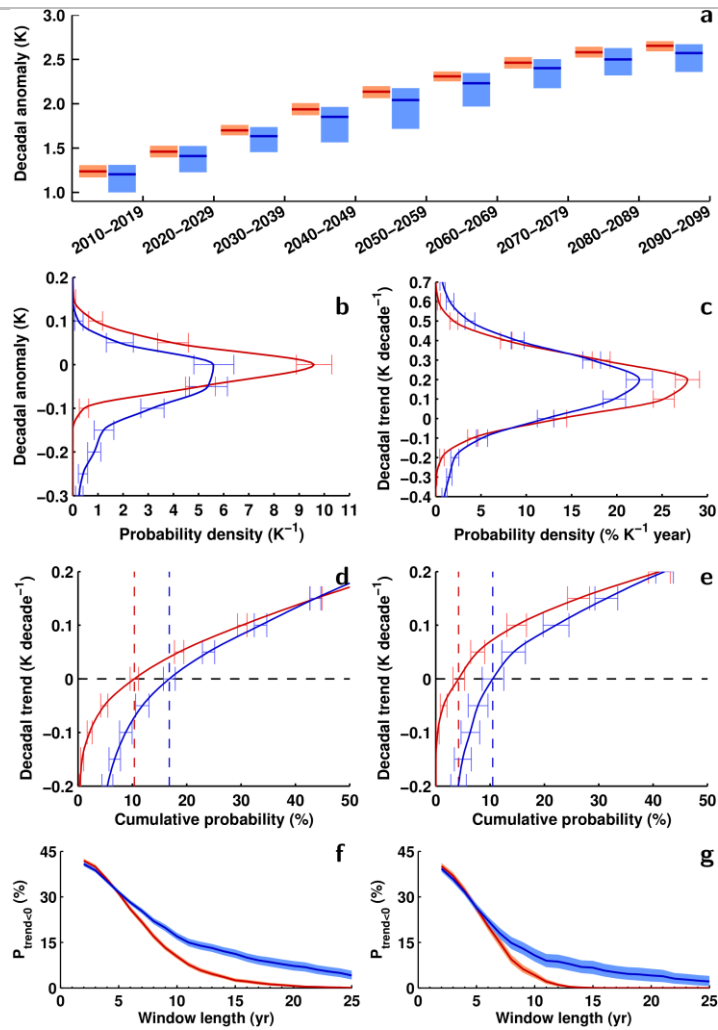
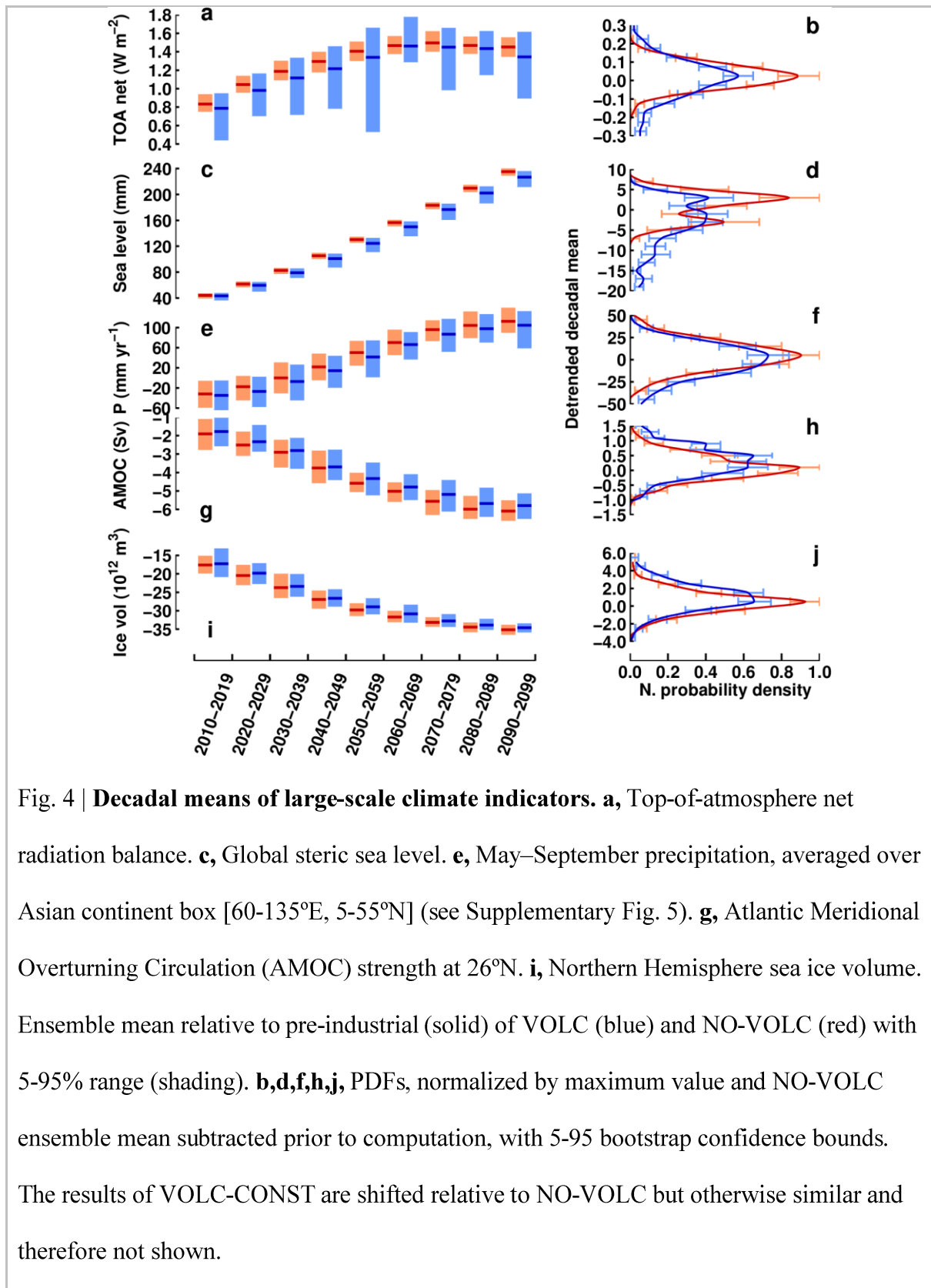


Fig. 3 | **Decadal temperature means and trends.** **a**, Decadal means of GMST relative to pre-industrial. Ensemble mean (solid) with 5-95% range (shading) of VOLC (blue) and NO-VOLC (red). **b**, PDF with 5-95% bootstrap confidence bounds of decadal anomalies (without overlap) relative to NO-VOLC ensemble mean. **c**, As **b**, but for decadal trends. **d**, Cumulative probability distribution with 5-95% confidence bounds for decadal trends (with overlap), using a 10-year window that is moved over 2006–2099. **f**, Probability for obtaining negative trends as function of length (solid) with 5-95% bootstrap confidence bounds (shading). **e,g**, As **d,f**, but for the shorter period 2006–2050.



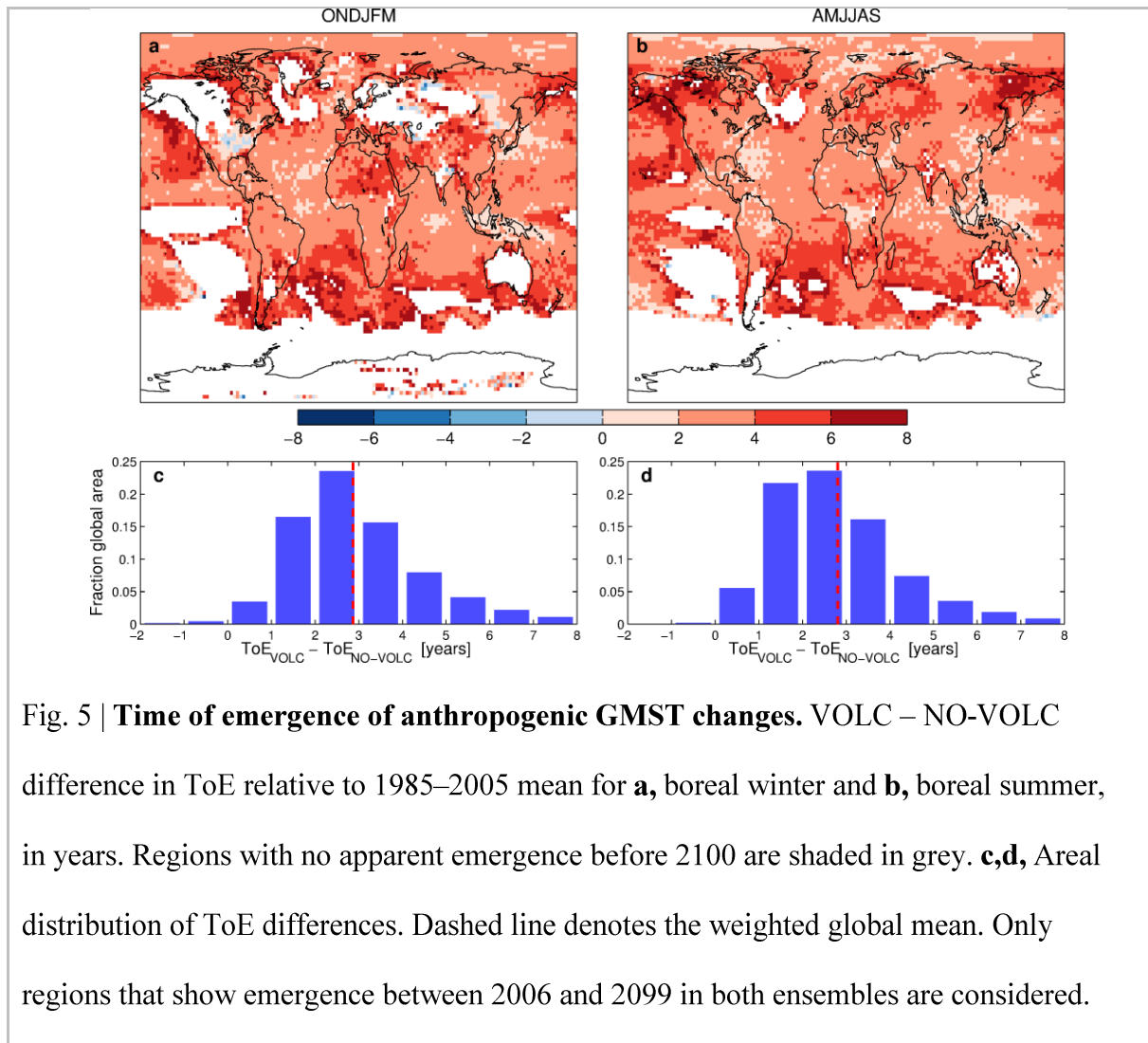


Fig. 5 | Time of emergence of anthropogenic GMST changes. VOLC – NO-VOLC difference in ToE relative to 1985–2005 mean for **a**, boreal winter and **b**, boreal summer, in years. Regions with no apparent emergence before 2100 are shaded in grey. **c,d**, Areal distribution of ToE differences. Dashed line denotes the weighted global mean. Only regions that show emergence between 2006 and 2099 in both ensembles are considered.

469 Acknowledgements

470 We thank XXX. This study was funded by YYY.

471 Individual author contributions

472 S.O., P.T. and I.B. developed the stochastic forcing model. S.W. and M.S. helped with the
473 utilisation and interpretation of the ice-core reconstructions. I.B., P.T., S.O. and E.H.
474 conceived and designed the simulation experiments. E.H. performed the ToE analysis. All
475 authors contributed to writing the manuscript.